Three-Dimensional Analysis of Eddy Current and Electromagnetic Force in Cold Crucibles

H. Tsuboi, M. Tanaka and T. Misaki
Department of Information Engineering
Fukuyama University
Gakuencho, Fukuyama 729-02, Japan

T. Naito
Fuji Electric Corporate R & D, Ltd.
Ichihara, Chiba 290, Japan

Abstract **- Three-dimensional eddy current distributions in cold crucibles are analyzed by using an integro-differential method. The electromagnetic force is calculated from the obtained eddy current distributions. In this paper, computations of eddy current and levitation force of the molten metal in some cold crucible models are performed, and the influences of coil position, the number of segments of the crucible, frequency of the coil current and gap length between the segments on the levitation force are discussed. Furthermore, an experimental verification is presented.**

I. Introduction

A cold crucible in which molten metal is levitated is useful equipment for melting metal without contamination. The cold crucible is composed of several segments. Eddy currents are induced on the surface of the crucible and the molten metal by high frequency currents in the coils around the crucible. The molten metal is levitated by the Lorentz force of the eddy current. For the design of the cold crucible, we have to know the distribution of the eddy currents on the surfaces of the crucible and the molten metal. The levitation force and the Joule heat are evaluated from the eddy current distributions.

In the case of a small penetration depth, the eddy current distributions can be calculated by an integro-differential method using an electric vector potential where the active parts of the conductor are approximated by thin conducting sheets [1-4]. The eddy current distributions on the surface of the crucible and the molten metal are calculated by an integro-differential method [5]. In this paper, the eddy current distribution is calculated and the levitation force of the molten metal is obtained from the eddy current. The influences of the coil position, the number of segments of the crucible, frequency of the coil currents and the gap length between the segments on the levitation force are investigated, and an experimental verification is shown.

Manuscript received November 1, 1993.

II. Integro-Differential Method

When the penetration depth is small and the active parts of the conductor can be approximated by thin conducting plates, the integro-differential equation for the normal component of the electric vector potential T is obtained as follows:

$$\frac{1}{\sigma}\nabla^2 T = \frac{j\omega\mu_0 h}{4\pi}\iint_S \frac{\{\nabla\times(\boldsymbol{n}T)\}\times\boldsymbol{r}\cdot\boldsymbol{n}}{r^3}\,ds + j\omega\boldsymbol{B}_S\cdot\boldsymbol{n} \tag{1}$$

where $\boldsymbol{n}$ is the unit normal vector, $\boldsymbol{B}_S$ is the magnetic flux density by the external sources, h is the thickness of the active parts and S is the surface of the conducting bodies.

The eddy current density $\boldsymbol{J}$ is calculated by

$$\boldsymbol{J} = \nabla\times\boldsymbol{T}. \tag{2}$$

The Lorentz force $\boldsymbol{f}$ and the levitation force F are calculated by

$$\boldsymbol{f} = \{\nabla\times(\boldsymbol{n}T)\}\times\boldsymbol{B}^* \tag{3}$$

$$F = \left(h\iint_S \boldsymbol{f}\,ds\right)_z \tag{4}$$

where * denotes complex conjugation.

III. Computation Models and Results

Two cold crucible models are shown in Fig. 1 [6], [7]. The molten metal is approximated by a sphere whose conductivity is 2×10^7 S/m. The conductivity of the crucible is 5×10^7 S/m. In the model B, the

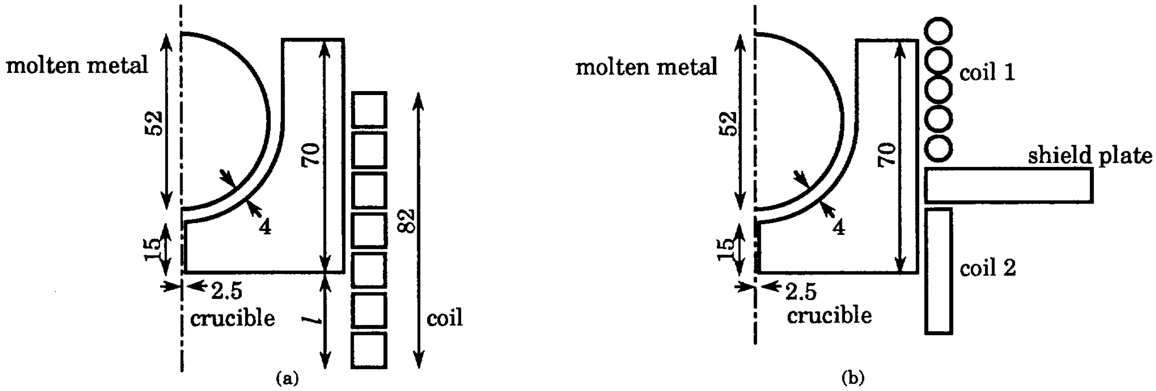

Fig. 1. Cold crucible models, (a) model A, (b) model B.

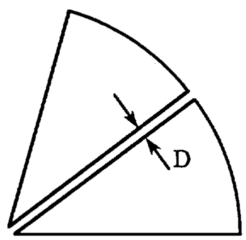

Fig. 2. Definition of the gap length between the segments of the crucible.

frequencies of the currents applied to upper and lower coils are different. The input power and the frequency of each coil are controlled individually to stabilize the motion of the molten metal.

In the model A, the crucible is divided into N segments (N = 24). The frequency of the coil current f is 3 kHz. The gap length between segments D, whose definition is shown in Fig. 2, is 0.5 mm. The arrangement of triangular elements is shown in Fig. 3, where the number of triangular elements is 4512. The numbers of triangular elements for a segment of the crucible and the sphere are 144 and 1056, respectively. The region to be analyzed is reduced to one forty-eighth by rotational symmetry and reflective symmetry [8]. The number of unknowns is 71, and the computation time and the memory storage are about 50 minutes and 800 kbytes using SONY NEWS (17 MIPS): NWS 3260 with R3000, 20MHz.

Variations of the levitation force for the coil positions are shown in Fig. 4, where l is the distance between the coil bottom and the crucible bottom. The computed results agree with the experimental results.

Figure 5 shows the real parts of the equipotential lines on the surfaces of a segment of the crucible and the sphere in the model A (l = 30).

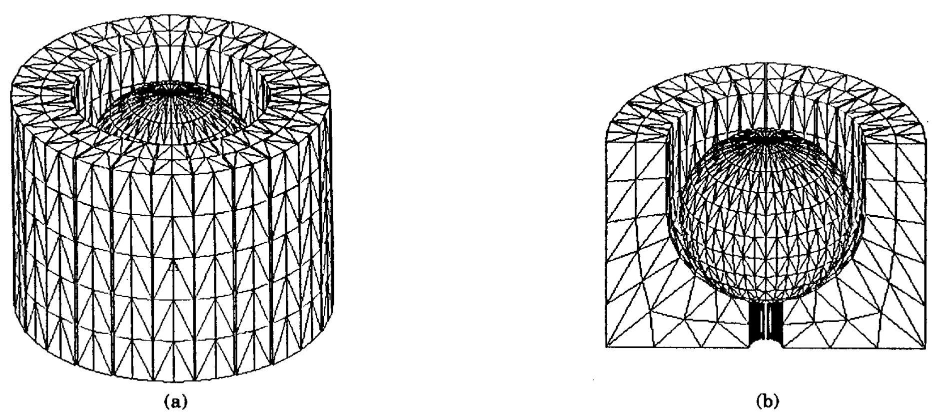

Fig. 3. Triangular mesh, (a) whole model, (b) a half of the crucible and the sphere.

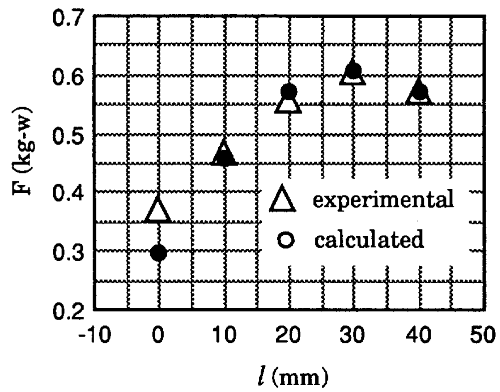

Fig. 4. Variations of the levitation force for the coil positions.

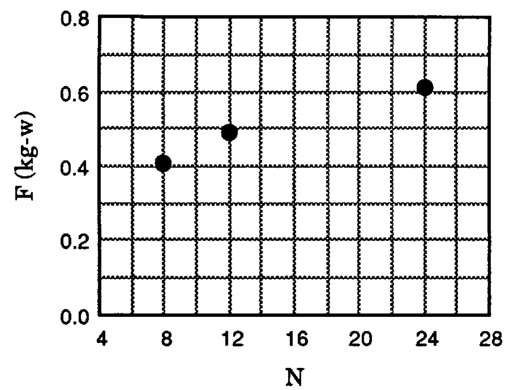

Fig. 7. Influence of the number of segments of the crucible.

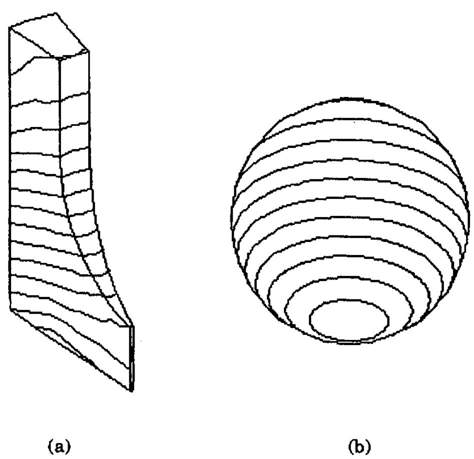

Fig. 5. Real part of the equipotential lines, (a) on the surface of a segment of the crucible, (b) on the surface of the sphere.

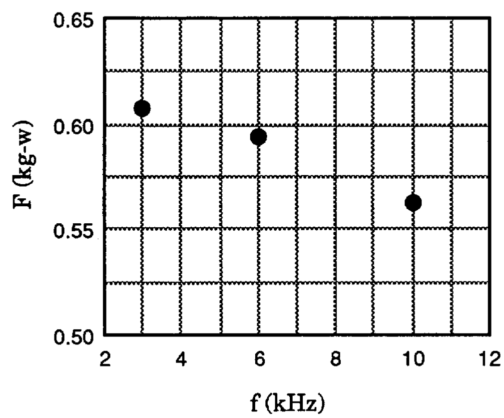

Fig. 8. Influence of the frequency of the coil currents.

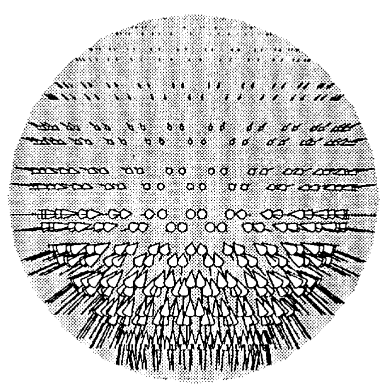

Fig. 6. Distribution of the electromagnetic force in the model A.

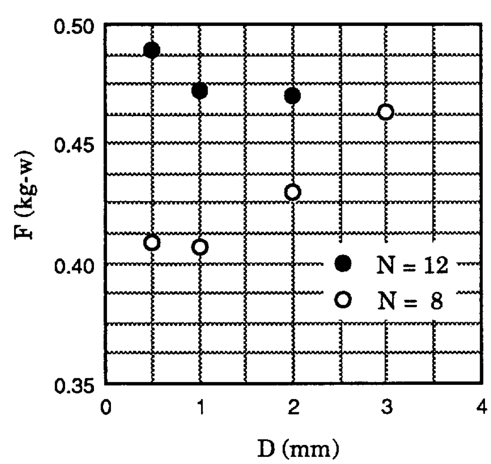

Fig. 9. Influence of the gap-length between the segments of the crucible.

Figure 6 shows the distributions of the Lorentz force on the surfaces of the crucible and the sphere. The influence of the number of segments on the levitation force is shown in Fig. 7 where $f = 3\,kHz$, l = 30 and D = 0.5. The levitation force increases with the number of segments N.

Figure 8 shows the levitation forces for the frequencies of the coil currents 3, 6 and 10 kHz, where l = 30, D = 0.5 and N = 24. The levitation force decreases with frequency of the coil currents. In this case, the coil currents are constant: 1000 A for each coil. However, the coil current decreases with the frequency for the same input power in practical crucible.

The influence of the gap length D between the segments on the levitation force is shown in Fig. 9. There is an optimal gap length D which is determined for the number of segments N.

Figure 10 shows the distribution of the Lorentz force on the surface of the sphere in model B. In this case, the computation was done without the shield plate shown in Fig. 1 (b), and the distribution of the electromagnetic force was calculated by superposing the forces caused by the coil 1 and the coil 2. The frequencies of the coil 1 and the coil 2 are 30 kHz and 3 kHz, respectively. The motion of the molten metal can be controlled by the two types of forces: one is the levitation force on the bottom surface caused by the coil 2 and another is the pressure on the upper and side surface of the molten metal caused by the coil 1.

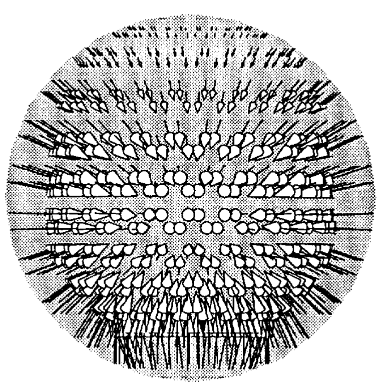

Fig. 10. Distribution of the electromagnetic force in the model B.

IV. Conclusion

The eddy current distributions were calculated by the integro-differential method using the approximation of current sheets for the active parts of the conductors in the cold crucible. The levitation force of the molten metal was obtained from the eddy current distribution. The influences of the coil position, the number of segments of the crucible, the frequency of the coil current and the gap length between the segment on the levitation force were investigated. The calculated levitation forces for some coil positions gave good agreement of the experimental results. Furthermore, the electromagnetic force of the two-frequency-type cold crucible was analyzed. The obtained results and the developed codes can be utilized to the optimal design of cold crucible systems.

References

[1] A. Nicolas, "3D Eddy Current Solution by BIE Techniques," *IEEE Trans. on Magn.*, Vol. 24, No. 1, pp. 130-134, 1988.

[2] S. J. Salon, B. Mathewson and S. Uda, "An Integro-Differential Approach to Eddy Currents in Thin Plates," *IEEE Trans. on Magn.*, Vol. MAG-19, No. 6, pp. 2405-2409, 1983.

[3] S. R. H. Hoole, *Computer Aided Analysis and Design of Electromagnetic Devices*, Elsevier, NY, 1989.

[4] C.J. Carpenter and E.A. Wyatt, "Efficiency of Numerical Techniques for Computing Eddy Currents in Two and Three Dimensions," *Proc. COMPUMAG, Oxford*, pp. 242-250, 1976.

[5] H. Tsuboi, M. Tanaka, F. Kobayashi and T. Misaki, "Three-Dimensional Eddy Current Analysis of Induction Melting in Cold Crucibles," *IEEE Trans. on Magn.*, Vol. 29, No. 2, 1993.

[6] K. Sakuraya, T. Watanabe, A. Fukuzawa, M. Yamazaki, T. Take, M. Fujita and T. Morita, "Measurement of Temperature in Cold Crucible," *ISEM-Nagoya*, paper No. BP-3-2, January 26-29, 1992.

[7] K. Sakuraya, T. Watanabe, A. Fukuzawa, T. Take and T. Morita, "The Influence of Slits of Cold Crucible and Frequency on the Levitation Force," *CAMP-ISIJ*, Vol. 4-963, 1991 (in Japanese).

[8] H. Tsuboi, A. Sakurai and T. Naito, "A Simplification of Boundary Element Model with Rotational Symmetry in Electromagnetic Field Analysis," *IEEE Trans. on Magn.*, Vol. 26, No. 5, pp. 2771-2774, 1990.